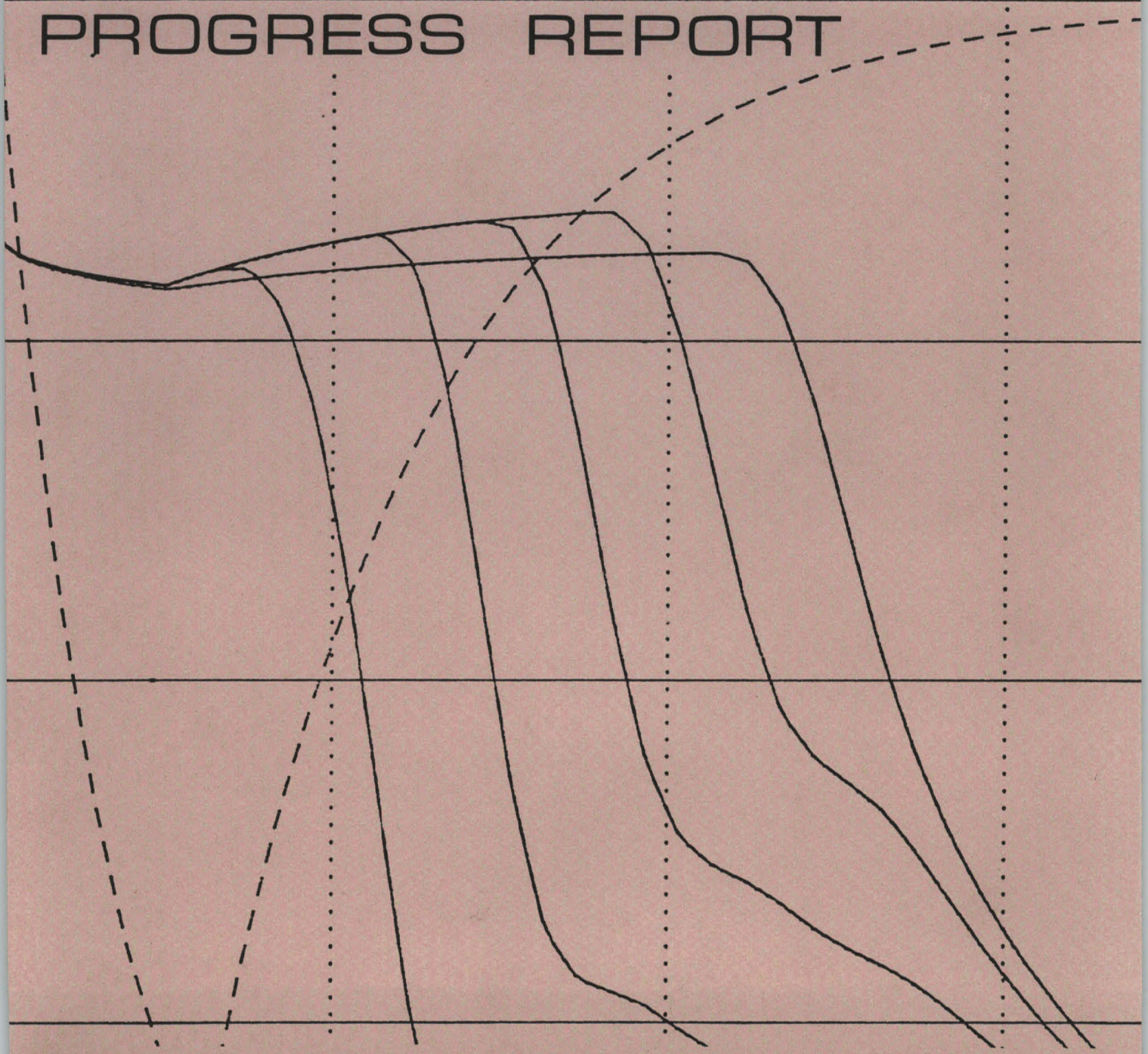


# **R** RESEARCH **L** LABORATORY of **E** ELECTRONICS

No. 126  
Jan. 1984

PROGRESS REPORT





**Massachusetts Institute of Technology**  
**RESEARCH LABORATORY OF ELECTRONICS**

**RLE PROGRESS REPORT No. 126**

**January 1984**

**Submitted by: J. Allen  
R. Birgeneau**

This report, No. 126 in a series of Progress Reports issued by the Research Laboratory of Electronics, contains the customary annual statement of research objectives and summary of research for each group. The report covers the period January 1, 1983–December 31, 1983, and the source of support is indicated for each project. On the masthead of each section are listed the academic and research staff and the graduate students who participated in the work of the group during the year. The listing of personnel in the back of the book includes only members of the laboratory during 1983.



## List of Figures

|                     |   |     |
|---------------------|---|-----|
| <b>Figure 3-1:</b>  | Two-Photon Absorption from 2s→3s in <sup>7</sup> Li   | 8   |
| <b>Figure 3-2:</b>  | Two-Photon Absorption from 2s→3s in <sup>6</sup> Li   | 8   |
| <b>Figure 3-3:</b>  | Enhanced absorption of blackbody radiation. Rydberg atoms are placed on the 32d state of sodium inside of a 77 K cavity. As the cavity is tuned on resonance, transfer of population from the 32d to the 33p state is observed. The transfer rate is increased on resonance by a factor of 10 <sup>4</sup> , the Q of the cavity. Total transfer is limited by collective atom effects inside the cavity. <sup>2</sup>  | 10  |
| <b>Figure 3-4:</b>  | A novel detection scheme is employed for determining the final state of the Rydberg atom. A set of field plates are tipped with respect to one another by 5°. As the atom drifts into the detection region it experiences an increasing field until it ionizes. The position and time of the resulting electron is recorded by an array of collector strips. The position determines the final states of the atom and the time determines the velocity of the atom. | 11  |
| <b>Figure 3-5:</b>  | Comparison of the shape of experimental and theoretical resonance profiles for four photon multiphoton ionization of atomic hydrogen. Note that the power density used to generate the theoretical profile is not the same as the power density used for the experimental profile.  | 12  |
| <b>Figure 3-6:</b>  | Differential cross section for Δj = 16, obtained by procedure described in paper submitted to J. Chem. Phys.  | 14  |
| <b>Figure 3-7:</b>  |   | 15  |
| <b>Figure 3-8:</b>  |   | 15  |
| <b>Figure 3-9:</b>  |   | 17  |
| <b>Figure 3-10:</b> |   | 18  |
| <b>Figure 3-11:</b> |   | 18  |
| <b>Figure 8-1:</b>  | Probe Lineshape as a Function of Frequency for a Pump Intensity of 4 W/cm <sup>2</sup> :  | 43  |
|                     | (a) detector size large than probe beam diameter  |     |
|                     | (b) detector size smaller than probe beam diameter  |     |
|                     | Frequency Scale: 560 kHz per large box  |     |
| <b>Figure 12-1:</b> | Trough Waveguide with alternating base asymmetry and field sampling probes (1 → H field, 2 → E field).  | 61  |
| <b>Figure 12-2:</b> | Relative power absorption for an infinite cylinder of muscle tissue   | 62  |
| <b>Figure 18-1:</b> | Analysis of global particle confinement   | 103 |
| <b>Figure 18-2:</b> | Parail-Pogutse instability observed by hard and soft x-ray diagnostics during LHCD  | 105 |
| <b>Figure 18-3:</b> | Spectra of the steady background emission at $\bar{n}_e = 4.5 \times 10^{12} \text{cm}^{-3}$ for (a) Ohmic (b) LHCD discharges  | 106 |
| <b>Figure 18-4:</b> | Spectra of the intense bursts of emission plotted in dB above the background emission level of $\bar{n}_e = 4.5 \times 10^{12} \text{cm}^{-3}$ for (a) Ohmic (b) LHCD discharges  | 107 |
| <b>Figure 18-5:</b> | Temporal evolution of the central ion temperature during rf injection with the top-launcher   | 108 |
| <b>Figure 18-6:</b> | The electron temperature, Te, derived from $2\omega_{ce}$ emission for a typical neutral beam heated ISX-B discharge at $B_0 = 13.1 \text{ kG}$ .   | 109 |
| <b>Figure 27-1:</b> |   | 206 |
| <b>Figure 27-2:</b> | Polarization of the ith Burst   | 215 |
| <b>Figure 27-3:</b> |   | 217 |
| <b>Figure 27-4:</b> | Result of Gaussian filter acting on single element and five-element letter  | 222 |

stripes, with identical degrees of blur. The vertical line marks the center of the stripe

**Figure 27-5:** Plot of size of Snellen letters and the new letters as a function of visual acuity of subject 223

# General Physics



